Fast-electron transport and heating of solid targets in high-intensity laser interactions measured by $K\alpha$ fluorescence

E. Martinolli,[1] M. Koenig,[1] S. D. Baton,[1] J. J. Santos,[1] F. Amiranoff,[1] D. Batani,[2] E. Perelli-Cippo,[2] F. Scianitti,[2]
L. Gremillet,[3] R. Mélizzi,[3] A. Decoster,[3] C. Rousseaux,[3] T. A. Hall,[4] M. H. Key,[5] R. Snavely,[5] A. J. MacKinnon,[5]
R. R. Freeman,[6] J. A. King,[5] R. Stephens,[7] D. Neely,[8] and R. J. Clarke[8]

[1]*Laboratoire pour l'Utilisation des Lasers Intenses, UMR7605, CNRS-CEA-Université Paris VI-Ecole Polytechnique,
91128 Palaiseau, France*
[2]*Dipartimento di Fisica "G. Occhialini," Università di Milano-Bicocca, Piazza della Scienza 3, 20126 Milano, Italy*
[3]*Commissariat à l'Energie Atomique-DAM, Bruyères-le-Châtel, France*
[4]*University of Essex, Colchester CO4 3SQ, United Kingdom*
[5]*Lawerence Livermore National Laboratory, Livermore, California, USA*
[6]*University of California Davis, Davis, California, USA*
[7]*Inertial Fusion Technology Division, Energy Group, General Atomics, San Diego, California 92121, USA*
[8]*Central Laser Facility, Rutherford Appleton Laboratory, Chilton, United Kingdom*
(Received 9 May 2005; revised manuscript received 21 November 2005; published 17 April 2006)

We present experimental results on fast-electron energy deposition into solid targets in ultrahigh intensity laser-matter interaction. X-ray $K\alpha$ emission spectroscopy with absolute photon counting served to diagnose fast-electron propagation in multilayered targets. Target heating was measured from ionization-shifted $K\alpha$ emission. Data show a 200 μm fast-electron range in solid Al. The relative intensities of spectrally shifted Al $K\alpha$ lines imply a mean temperature of a few tens of eV up to a 100 μm depth. Experimental results suggest refluxing of the electron beam at target rear side. They were compared with the predictions of both a collisional Monte Carlo and a collisional-electromagnetic, particle-fluid transport code. The validity of the code modeling of heating in such highly transient conditions is discussed.

The transport of laser-accelerated relativistic electrons in dense matter is a key issue for the fast-ignition approach to inertial confinement fusion [1]. In this scheme, a few kJ of fast electrons (FE) produced by an intense laser pulse should heat the dense deuterium and tritium (DT) fuel up to ignition temperature ($\approx$10 keV over $\approx$10 μm size). It is therefore critical to estimate the amount of energy that may be carried and deposited by the electrons at a given depth into the target. Moreover, understanding relativistic electron transport is a prerequisite for many applications of ultraintense lasers, notably proton acceleration from solids [2].

Over the past few years, FE transport into solids has been experimentally investigated by means of optical [3], x-ray [4–6], proton diagnostics [7,8]. Even though substantial results have been obtained concerning the presence of FE jets, the directionality of the beam, and the self-generated magnetic and electric fields associated with the FE current, a complete picture of the propagation phenomena is still missing. In particular, only a few experiments aimed at a quantitative study of the FE energy deposition and induced heating *inside* the target [6]. In this respect, x-ray diagnostics stand out as the only ones capable of providing a direct insight into this process. By contrast, optical diagnostics at target rear side (self-emission, reflectivity) only allow indirect measurements (further hampered by the possibility of thermal emission at early times being blinded by an intense optical transition radiation [9,10]).

This paper presents quantitative in-depth measurements of temperature *inside* multilayered targets, by using the $K\alpha$ emission induced by FE. Two different fluorescer layers (Cu and Al) placed at different depths behind an Al *propagation* foil (see Fig. 1) provided absolute $K\alpha$ yields from which one can infer FE temperature [11] and laser-to-electron energy conversion [5]. We also detected the spectrally shifted $K\alpha$ lines from the Al fluorescer. The partial ionization due to the FE-induced heating lowers the screening of the nucleus by the bound electrons and entails a blueshift by several tens of mÅ of the $K\alpha$ line [12]. The relative intensity of the shifted lines then enables one to estimate the ionization state and the background temperature (these diagnostics were previously used in ns-laser FE experiments [13]). Results were compared with simulations from a Monte Carlo transport code and the hybrid collisional-electromagnetic code PÂRIS [14].

The same experiment made use of complementary diagnostics such as time-resolved rear-side optical imaging and x-ray $K\alpha$ imaging, whose results are described in other papers [6,10].

The CPA Vulcan laser (850 fs, 1.057 μm, 35–40 J *on target*) was focused at normal incidence by a f/3.5 off-axis
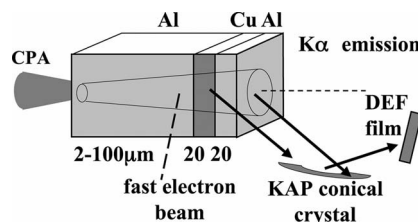

FIG. 1. Experimental setup for $K\alpha$ spectroscopy of Al and Cu fluorescent layers buried into multilayered targets.
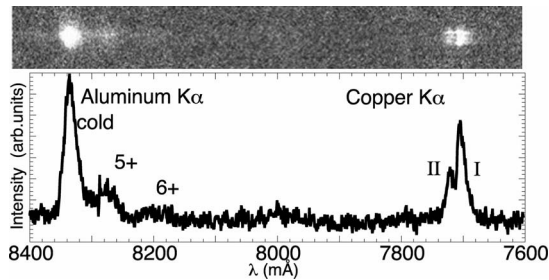
FIG. 2. Spectrum from an Al_11-Cu_25-Al_16 μm target. Left: Al $K\alpha$ and hot shifted lines. Right: double-peak cold Cu $K\alpha$ line.
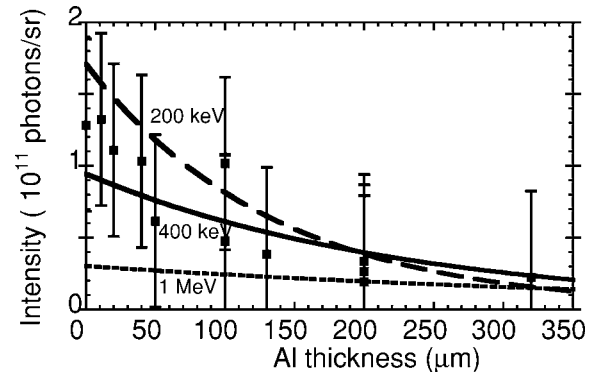

FIG. 3. $K\alpha$ intensity from the Cu layer vs front aluminum thickness: experimental data (solid squares) and Monte Carlo simulations for three different beam temperatures and without refluxing (lines).

parabolic mirror onto a flat multilayered target, as shown in Fig. 1. The small focal spot [≈ 15 μm full width at half maximum (FWHM)] allows an irradiance $\approx 1-5 \times 10^{19}$ W/cm^{-2}. About 10–20% of the laser energy is expected to be transferred to electrons accelerated up to several hundred keV [5,15]. The amplified spontaneous emission contrast ratio was $\approx 10^{-6}$, yielding a maximum intensity of 10^{13} W/cm^{-2} over 2 ns. Hydrodynamic simulations indicate that ASE should not affect targets thicker than 20 μm. Apart from ASE, no significant prepulse was present.

The target is typically composed of three layers. The front *propagation* layer is made of aluminum of thickness in the range 10–300 μm. Two 20 μm-thick fluorescers were placed behind the front layer. The first one is made of copper, whose bright 8.048 keV $K\alpha$ line is detectable at the fifth order (at 1.5 Å) by our spectrograph. This layer also entirely blocks the x-rays coming from the Al propagation layer. The second fluorescer is aluminum and emits the cold (1.487 keV) and spectrally shifted $K\alpha$ lines at 8 Å. Photoionization of the Al layer by the x-rays generated in the Cu layer was also considered and shown to be negligible in our case. The Cu layer was thermally bonded onto the Al front layer so as to avoid any glue or vacuum gap at the interface likely to disturb FE propagation.

The weak intensity of the shifted lines in the expected range of temperature [16] and the high noise level due to bremsstrahlung demanded a good photon collection efficiency as well as a high signal-to-noise (S/N) ratio. To this end, we designed a Bragg spectrograph based on a potassium-acid-phthalate (KAP) conically bent crystal [17], which provides a high brightness and a good spectral resolution over a wide spectral range (7–8.5 Å, including the $K\alpha$, the Heα, and Lyα lines). The integrated reflectivity of the crystal was absolutely calibrated using a tantalum-cathode x-ray source at energies corresponding to both Cu and Al $K\alpha$ lines.

Figure 2 shows the Al $K\alpha$ line (left side of the spectrum) as well as the first shifted line, which corresponds to the 5 + ionization state (*F*-like). The second shifted line, 6+, is weaker and almost merged with the background. The shifted lines up to the Al 4+ transitions are blended in the big *cold* peak. The cold Cu $K\alpha$ I and II lines are prominent at the right side. From their separation (≈ 19 mÅ), we deduce a spectral resolution of at least 500, as expected. The absolute intensity of the cold Cu line for the whole series of shots on multilayered targets is plotted versus the thickness of the

front layer in Fig. 3. The Al cold $K\alpha$ line (not shown) exhibits a similar exponential decay to that of the copper $K\alpha$ line. From the variation of the intensity of both the Cu and Al cold $K\alpha$ lines versus depth, we estimated the penetration range of the FE as 220 ± 30 μm.

Assuming a purely collisional propagation [18], the absolute values of $K\alpha$ yield (number of photons per steradian) depend both on FE beam temperature and energy (which for a given temperature is proportional to the number of FEs). On the other hand, the range inside the target and the intensity ratio from the two fluorescers is sensitive only to the beam temperature.

A full scale three-dimensional (3D) numerical description of the experiment accounting for both collisional and electromagnetic effects is currently out of reach from both the modeling and the computational points of view. First, in order to get a zero-order estimation of the FE *source* we used a Monte Carlo code retaining the actual spatial scale and the sole collisional processes. In this code [14] FE are deflected via random sampling of the screened Coulomb scattering cross section and slowed down via the average Bethe-Bloch stopping power formulas. $K\alpha$ photons [28] are calculated along each trajectory. The target remains cold and unperturbed during propagation. We assumed a collimated FE source with a relativistic Maxwellian distribution. We adjusted the beam total energy and temperature to reproduce the observed data (Fig. 3), neglecting reflection at boundaries (*single pass*). The range is best fitted with a temperature ≈ 400 keV (i.e., a mean energy ≈ 300 keV), in agreement with the main scaling laws reported in literature [19,20].

However, these simulations lead to discrepancies: the Cu/Al intensity ratio (see Fig. 4) is overestimated as compared to experimental absolute $K\alpha$ yields, giving a different laser-to-electron energy conversion efficiency whether one considers Cu (25%) or Al (50%). This behavior seems to suggest that some electrons are reflected into the target by the rear-side Debye sheath [21,22]. Refluxing would indeed increase the yield from the second fluorescer (Al), while the *exhausted* electrons may be unable to reach the first fluorescer layer (Cu) again.

In order to check the refluxing scenario in the context of our Monte Carlo field-free model, we performed *multipass*
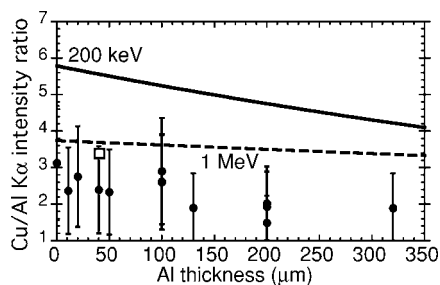
FIG. 4. Cu/Al $K\alpha$ ratio vs front aluminum thickness: experimental data (solid circles) compared with two Monte Carlo simulations both without refluxing for two beam temperatures (solid and dashed line) and with one PÂRIS code simulation (empty square).

simulations by *simply* adding reflective boundary conditions on FEs either at the rear side (simple refluxing) or at both the rear and front sides (multiple refluxing) as limiting cases of more complex situations. With refluxing, the experimental Cu/Al ratio can be correctly reproduced, as well as the penetration range. The energy conversion is reduced down to 8% in the multiple refluxing case and becomes consistent with both Al and Cu $K\alpha$ yields.

Special targets with fixed front Al Cu layers and a rear Al layer of variable thickness served to experimentally support the refluxing scenario: without refluxing, increasing the rear-layer thickness should only slightly reduce the Cu $K\alpha$ signal via the absorption of emitted x-rays. Instead, if significant refluxing takes place, the reduction must be stronger since less recirculating electrons can reach the Cu layer, being absorbed in the thicker rear layer. The experimental results shown in Fig. 5 imply that the real situation lies probably somewhere between the limiting cases of single-pass (no refluxing) and multiple refluxing, with an energy efficiency and a temperature respectively in the range 8–15% and close to 400 keV.

The Al $K\alpha$ 5+ (O-like) shifted line is visible from targets with a front layer thickness up to 100 μm, whereas the 6+ (N-like) line is detectable only from the thinnest targets, or those with no intermediate Cu layer. The experimental intensity ratio of the hot 5+ $K\alpha$ line to the cold one (Fig. 6, right) is 0.2 and does not show any particular trend versus Al thickness. Shifted lines arise from ionization of the emitting atoms. Given the negligible role of photoionization of the Al layer, the ionization must be related to the temperature increase due to the electron beam energy deposition. We therefore used the atomic physics code UBCAM [23] to compute
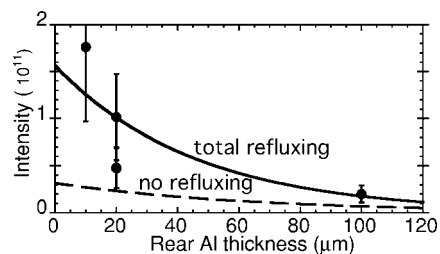

FIG. 5. Cu $K\alpha$ intensity vs Al rear layer thickness: experimental data (solid circles) and Monte Carlo simulations, with (solid line) and without (dashed line) electron refluxing.

the ionic fractions of solid aluminum heated up to a few ten eV in local thermodynamic equilibrium (LTE) conditions. The 4+ state (corresponding to the 5+ line) appears to progressively account for up to 20% of the cold line intensity when the target is heated up to 20 eV. At the same time, the absence of a significant 6+ line suggests a temperature lower than about 30 eV.

Yet, the actual experimental situation is complicated by several effects, which led us to step up to another level of modeling beyond the limitations of our simple collisional Monte Carlo code. First, the size of the strongly heated region at the target rear side may be substantially narrower than the transverse spread of the FE beam: $K\alpha$ photons originating from peripheral colder regions will only contribute to the cold peak, hence lowering the space-integrated measured line ratio. Second, one must consider that FEs both heat the target and produce $K\alpha$ photons (i.e., here the *pump* coincides with the *probe*). Hence, any finite time between energy deposition and temperature rise will dramatically affect the production of *hot* $K\alpha$ photons. Put in other terms, the relaxation time needed to significantly heat the bulk material might be too long with respect to the duration of the electron pulse itself: in this case, too few electrons would remain to detect and thus diagnose the final heating level. However, refluxing might downplay this effect by effectively increasing the FE transit time scale through the target.

A further, more fundamental, complication regards the heating process itself. As is now well known, the energy deposition, and thus the ionization, stems both from the collisions undergone by the FEs and the ohmic dissipation of the resistive, inductively driven return current [24]. These two mechanisms have been recently modeled by so-called hybrid, collisional-electromagnetic transport codes [24,25]. "Hybrid" refers to the assumption that fast- and thermal-electron populations can be treated separately, the former being modeled as kinetic macroparticles subject to both the Lorentz force and collisions, and the latter as a resistive, massless fluid. The resulting suppression of the high space and time frequencies of the dense target response offers computational advantages compared with standard particle-in-cell (PIC) codes, but the range of validity of this approximation is still unclear. Yet, the fluid model shifts the emphasis onto the conductivity, which is not well known both theoretically and experimentally in the solid density, low-temperature regime, let alone if thermal equilibrium no longer holds due to the few-ps electron-ion (e-i) energy relaxation. Moreover how this nonequilibrium (characterized by $T_e \gg T_i$) affects the joule effect is still unclear because of the uncertain contribution of the electron-electron (e-e) interactions to the conductivity in the solid and liquid phases. In the context of fs laser-metal interaction, Eidmann *et al.* [25] have considered that the total collision frequency is solely governed by the e-i interactions, thus scaling as $\nu \propto T_i$, whereas [26,27] define a threshold electron temperature T_* $\sim (\varepsilon_F T_i / k_B)^{1/2}$ (where ε_F and k_B are respectively the Fermi energy and the Boltzmann constant) above which the e-e collisions prevail, yielding a dramatically modified scaling $\nu \propto T_e^2$.

In order to describe these highly transient and intertwined processes within a realistic configuration, we supplemented
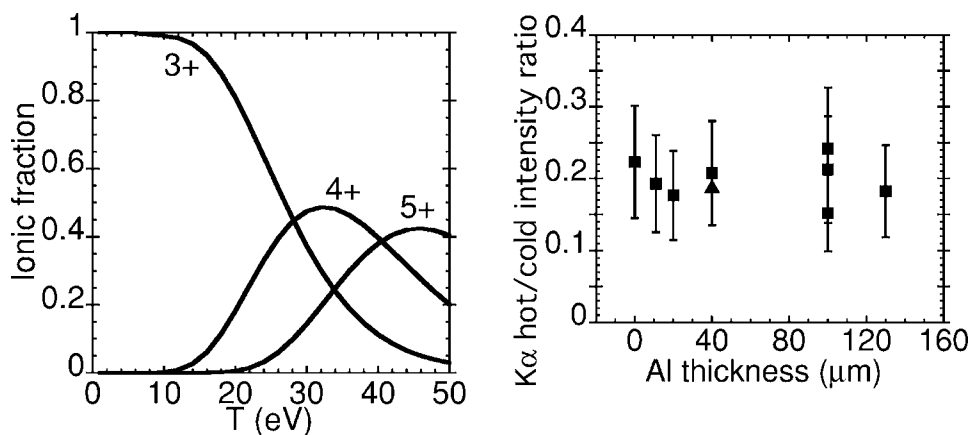
FIG. 6. Left: ion populations in solid Al vs temperature, calculated with the UBCAM atomic physics code. Right: experimental line ratio 5+/cold vs thickness for Al-Cu-Al targets (squares). We note that "5+" line corresponds to "4+" state. The triangle is the result of the PÂRIS code simulation described in the text.

the 3D PÂRIS hybrid transport code [14] by a new atomic physics model. T_e and T_i are calculated from the total deposited energy (ohmic and collisional) by a time-dependent model [25] neglecting thermal conduction. The energy is first transferred to the thermal electrons and then relaxed to the ions. Mean ionization as well as specific energies are interpolated on-the-fly from data tables precomputed by the average-atom code NOHEL [29]. The e-i coupling factors in Al and Cu are assumed constant and taken respectively from Refs. [25,30]. The conductivity is calculated from the total collision frequency by summing the e-i and e-e collision frequencies relevant for a given phase. The former is given by the Lee and More model in the whole temperature range [31], while the latter is computed from the formula derived in Ref. [32] in the plasma phase and the approximation $\nu_{ee} = (k_B T_e)^2 / \hbar \varepsilon_F$ [26] in the solid/liquid phases. To calculate on-the-fly the $K\alpha$ line emission [28], the local Al ionic fractions for K shell levels are interpolated at each time step from data tables precomputed by UBCAM code [23]. Mean ionization from UBCAM and NOHEL are consistent. FEs are injected as a drifting 3D relativistic Maxwellian distribution with temperature and drift velocity chosen so as to yield a mean energy and an angular divergence respectively close to 500 keV and ±20°. The incoming current profile is Gaussian in space and time (0.8 ps and 20 μm FWHM). Simple front and rear surface reflection mimics refluxing, an electrostatic model of the FE breakout into vacuum being currently not available in PÂRIS [33].

Figure 7 shows two-dimensional (2D) maps of T_e and T_i obtained at the end of a 2 ps simulation, that is, 1.2 ps after the pulse maximum, for an initially cold ($T_e=T_i=300$ K) 40 μm Al-20 μm Cu-20 μm Al target. The beam carries a total kinetic energy of 15 J, which corresponds to a 37% conversion efficiency, a value more than twice the one previously derived from the purely collisional model. The reason is that here collisions and inductive effects contribute almost evenly to the total beam slowing down. Even though only 55% of the incident energy has been absorbed by then, T_e should not increase much later on owing to the beam dilution, as opposed to T_i slowly rising up to equilibrium. Heating appears to be mostly confined close to the front surface. Near the rear side, rather modest temperatures are

attained: T_e reaches $\approx$25 eV over a 100 μm spot whereas T_i does not exceed $\approx$5 eV. The resulting Cu/Al and hot/cold Al $K\alpha$ ratios are respectively 3.4 and 0.19, in good agreement with the experimental values. We tried to assess the influence of the target e-e collisions by running a simulation retaining the sole e-i contribution to the resistivity. The final temperature map in this case remains similar to that of the previous simulation but with a slower heating rate due to the initial dependence of the resistivity on T_i. Consequently, the hot/cold $K\alpha$ ratio drops to 0.09. By rapidly increasing the initial heating rate, the e-e interactions thus seem to account for the relatively large experimental hot/cold $K\alpha$ ratio.

In this paper we have studied the heating of a solid multilayered target by a laser-generated distribution of relativistic electrons via x-ray $K\alpha$ fluorescence emission spectroscopy. Experimental results are consistent with a 200 μm FE range in solid Al and a temperature rise of a few ten eV up to a 100 μm depth. These results are satisfactorily reproduced by hybrid transport simulations which go beyond the limitations of a simple collisional (Monte Carlo) modeling. They pinpoint the importance of an accurate description of the highly transient electrical properties of the heated material. In particular, they seem to evidence the role of e-e interactions in the target response. Our data also appear to support the occurrence of a partial refluxing of the electron
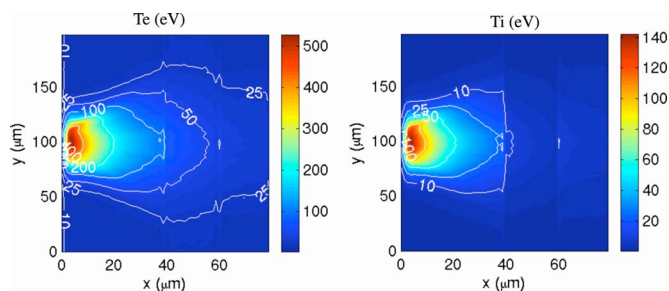

FIG. 7. (Color online) 3D PÂRIS simulation: 2D longitudinal slices of target T_e (left) and T_i (right) at 2 ps after the beginning of the FE pulse.

beam.

Let us finally emphasize that our measured heating (≤ 30 eV) roughly corresponds to 1 eV per joule of laser energy on solid-density target. A similar result has been obtained in Osaka [34] using about 300 J of laser-input energy in an integrated implosion experiment. Although extrapolations to a real inertial confinement fusion (ICF) regime are quite questionable, this seems to provide substantial grounds for fast ignition, whose demonstration should be within the reach of a 10 kJ-class short laser pulse.

[1] M. Tabak *et al.*, Phys. Plasmas **1**, 1626 (1994).

[2] A. J. Mackinnon, M. Borghesi, S. Hatchett, M. H. Key, P. K. Patel, H. Campbell, A. Schiavi, R. Snavely, S. C. Wilks, and O. Willi, Phys. Rev. Lett. **86**, 1769 (2001).

[3] L. Gremillet *et al.*, Phys. Rev. Lett. **83**, 5015 (1999).

[4] M. Santala *et al.*, Phys. Rev. Lett. **84**, 1459 (2000).

[5] F. Pisani *et al.*, Phys. Rev. E **62**, R5927 (2000).

[6] R. B. Stephens *et al.*, Phys. Rev. E **69**, 066414 (2004).

[7] M. Borghesi *et al.*, Phys. Rev. Lett. **92**, 055003 (2004).

[8] A. J. Mackinnon *et al.*, Rev. Sci. Instrum. **75**, 3531 (2004).

[9] J. J. Santos *et al.*, Phys. Rev. Lett. **89**, 025001 (2002).

[10] S. Baton *et al.*, Phys. Rev. Lett. **91**, 105001 (2003).

[11] T. Hall *et al.*, Phys. Rev. Lett. **81**, 1003 (1998).

[12] L. L. House, Astrophys. J., Suppl. **18**, 21 (1969).

[13] J. D. Hares, J. D. Kilkenny, M. H. Key, and J. G. Lunney, Phys. Rev. Lett. **42**, 1216 (1979).

[14] L. Gremillet *et al.*, Phys. Plasmas **9**, 941 (2002).

[15] M. Key *et al.*, Phys. Plasmas **5**, 1966 (1998).

[16] A. Rousse, P. Audebert, J. P. Geindre, F. Fallies, J. C. Gauthier, A. Mysyrowicz, G. Grillon, and A. Antonetti, Phys. Rev. E **50**, 2200 (1994).

[17] E. Martinolli *et al.*, Rev. Sci. Instrum. **75**, 2024 (2004).

[18] R. J. Harrach and R. E. Kidder, Phys. Rev. A **23**, 887 (1981).

[19] F. N. Beg *et al.*, Phys. Plasmas **4**, 447 (1997).

[20] S. Wilks, Phys. World **5**, 26 (1992).

[21] A. J. Mackinnon *et al.*, Phys. Rev. Lett. **88**, 215006 (2002).

[22] S. C. Wilks *et al.*, Phys. Plasmas **8**, 542 (2001).

[23] G. Chiu and A. Ng, Phys. Rev. E **59**, 1024 (1999).

[24] J. R. Davies, A. R. Bell, M. G. Haines, and S. M. Guerin, Phys. Rev. E **56**, 7193 (1997).

[25] K. Eidmann, J. Meyer-ter-Vehn, T. Schlegel, and S. Huller, Phys. Rev. E **62**, 1202 (2000).

[26] A. P. Kanavin, I. V. Smetanin, V. A. Isakov, Y. V. Afanasiev, B. N. Chichkov, B. Wellegehausen, S. Nolte, C. Momma, and A. Tunnermann, Phys. Rev. B **57**, 14698 (1998).

[27] D. Fisher, M. Fraenkel, Z. Henis, E. Moshe, and S. Eliezer, Phys. Rev. E **65**, 016409 (2001).

[28] H. Kolbenstvedt, J. Appl. Phys. **38**, 4735 (1967).

[29] C. Bowen *et al.*, J. Quant. Spectrosc. Radiat. Transf. **81**, 71 (2003).

[30] B. Rethfeld *et al.*, Phys. Rev. B **65**, 214303 (2002).

[31] Y. Lee and R. More, Phys. Fluids **27**, 273 (1984).

[32] A. Decoster, *Modeling of Collisions* (Elsevier-Gauthier-Villars, Paris, 1998).

[33] M. Key *et al.*, IFSA, Kyoto (2001).

[34] R. Kodama, Nature **418**, 933 (2002).